

# Lactoferrin versus Dexamethasone in a Model of Acute Lung Injury in Adult Rat: Histological and Immunohistochemical Study

Original  
Article

Breehan A. Marzouk, Hanan A. Saleh, Sohier K. Ahmed and Doaa R. Sadek

Department of Histology, Faculty of Medicine, Ain Shams University, Cairo, Egypt

## ABSTRACT

**Introduction:** Acute lung injury (ALI) is one of the most dangerous illnesses affecting the lungs. During the COVID-19 pandemic, many patients developed ALI and ultimately lung failure. Local exposure to lipopolysaccharide (LPS) is associated with cytokine production by the lung resulting in the infiltration of neutrophils and other mononuclear cells. Lactoferrin (LF) is a glycoprotein that binds iron and may have anti-inflammatory properties.

**Aim of the Work:** To evaluate the possible therapeutic effects of lactoferrin versus dexamethasone (DEXA) on the structure of the lung in a model of lipopolysaccharide-induced acute lung injury in adult rats.

**Material and Methods:** Thirty-five adult male albino rats were divided randomly into 4 groups. Group I (control group), Group II (LPS group), Group III (LPS+LF group), Group IV (LPS+DEXA group). After 24 hours from the injections of both LF and DEXA, the lung specimens were processed for hematoxylin and eosin (H&E), periodic acid Schiff (PAS), orcein, toluidine blue, and immunohistochemical reaction for inducible nitric oxide (iNOS). Morphometric and statistical analysis were also done.

**Results:** H&E-stained sections of group II showed marked thickening of interalveolar septa (IAS) with heavy inflammatory cell infiltrations (neutrophils and macrophages). Most alveoli appeared narrowed and collapsed. Some bronchiolar epithelium appeared desquamated with cellular infiltration. A significant increase in the mean number of goblet cells and mast cells was detected. A disruption of elastic fibers was also noticed. A significant increased reaction to iNOS antibodies was also detected. On the other hand, the lung structure in group III and group IV showed significant improvement in all parameters.

**Conclusion:** Both lactoferrin and dexamethasone showed therapeutic and anti-inflammatory effects in LPS-induced ALI. These effects were more prominent in the dexamethasone group than the lactoferrin group as detected by microscopic, morphometric, and statistical studies.

**Received:** 14 December 2023, **Accepted:** 14 January 2024

**Key Words:** Acute lung injury, dexamethasone, iNOS, lactoferrin, lipopolysaccharide.

**Corresponding Author:** Doaa R. Sadek, MD, Department of Histology, Faculty of Medicine, Ain Shams University, Cairo, Egypt, **Tel.:** +20 10 0260 9026, **E-mail:** d.sadek@med.asu.edu.eg

**ISSN:** 1110-0559, Vol. 48, No. 1

## INTRODUCTION

Acute lung injury (ALI) is a common but under-recognized and undertreated disease in critical care medicine and has been associated with severe complications<sup>[1,2]</sup>. In the recent COVID-19 pandemic, many patients have developed acute respiratory distress syndrome (ARDS) with pulmonary edema and lung failure<sup>[3]</sup>.

Acute lung injury results in significant damage and inflammation of the lung tissue. Despite the great efforts to find new and/ or more active medicines to treat this condition, mortality still presents a high rate<sup>[4]</sup>.

Lipopolysaccharide is a component of the Gram-negative bacterial cell wall, which could induce a disturbance in the immune and inflammatory responses. Lipopolysaccharide consists of a lipid domain (hydrophobic) attached to a core oligosaccharide and a distal polysaccharide. Lipopolysaccharides are composed of three components

1. Lipid A: the hydrophobic domain, the primary virulence factor, and an endotoxin;

2. The repetitive hydrophilic distal oligosaccharide known as O-antigen;
3. The hydrophilic polysaccharide core<sup>[5]</sup>.

Administration of LPS has been shown to injure epithelial cell layers, induce epithelial cell apoptosis, and lead to the release of proinflammatory cytokines, chemotactic factors, and reactive oxygen species, which cause the aggregation of neutrophilic leukocytes, macrophages, and ultimately lung tissue injury<sup>[6]</sup>.

Lactoferrin is an iron-binding glycoprotein of the transferrin family that was first found in human milk<sup>[7]</sup>. Recent research has shown a growing interest in lactoferrin's potential as a preventive measure and an adjuvant treatment for many illnesses<sup>[8,9]</sup>.

Moreover, Dexamethasone is a potent, long-lasting synthetic glucocorticoid that possesses potent anti-inflammatory properties<sup>[10]</sup>. Although DEXA is widely used to treat various inflammatory diseases, it has many side effects and limitations<sup>[11]</sup>.

Nitric oxide (NO) is a molecule that is important in cellular signaling. It has several physiological functions including vasodilation, relaxation of smooth muscles, neurotransmission, and in the immune response<sup>[12]</sup>. Inducible NOS is expressed by many cell types such as infiltrating inflammatory cells, macrophages, T cells, neuroglial cells, and astrocytes<sup>[13]</sup>. Inducible NOS is distinct as it is not constitutively active but is induced by bacterial infection and pro-inflammatory cytokines, and therefore serves as part of the host immunological defense system. However, over-expression of iNOS and subsequently high NO levels could contribute to several diseases<sup>[14]</sup>.

### AIM OF THE WORK

This study aimed to compare the possible therapeutic role of LF versus DEXA on the microscopic structure of the lung in a model of LPS-induced ALI.

### MATERIALS AND METHODS

#### *Animals and ethical approval*

Thirty-five adult male albino rats were used in this study with a weight ranging from 180-200 gm. They were purchased from the Medical Ain Shams Research Institute (MASRI). Animals were housed in wire mesh cages at normal room temperature with water and food ad libitum. The Animal Ethical Committee of the Faculty of Medicine, Ain Shams University, provided general standards for the care and use of laboratory animals, which were followed for all animal procedures; the approval number is: FMASU: MS 681/ 2021.

#### *Chemicals*

- Lipopolysaccharide (LPS): (*Escherichia coli* 011: B4), was obtained from Sigma-Aldrich, Cairo, Egypt as a powder container (L2630-10 mg). The powder was dissolved in 4 ml saline and injected intraperitoneally (I.P) into the rats in a dose of (3mg/kg Body weight (B.W))<sup>[15]</sup>. Injection of LPS was used for induction of the ALI model.
- Lactoferrin (LF): Bovine lactoferrin (L9507-10MG) was obtained as a powder from Sigma-Aldrich, Cairo, Egypt. The solution for the injection was prepared by dissolving the powder in 0.5 ml saline and injecting I.P. into the rats (5mg/rat)<sup>[16]</sup>.
- Dexamethasone (DEXA): was obtained from AMRIYA Company as prepared ampoule 8mg/2ml. It was I.P. injected into rats (5mg/kg. B.W)<sup>[17]</sup>.

#### *Experimental design*

After seven days acclimatization period, 35 adult male albino rats were randomly classified into four groups:

**Group I (control group):** (20 rats), these rats were subdivided into four subgroups, 5 rats each.

- Subgroup IA: Rats received water and food ad libitum.

- Subgroup IB: Rats were injected I.P. with 0.2 ml saline.
- Subgroup IC: Rats were injected I.P. with LF (5mg/rat) dissolved in 0.2 ml saline<sup>[16]</sup>.
- Subgroup ID: Rats were injected I.P. with DEXA (5mg/kg B.W)<sup>[17]</sup>.

**Group II (LPS- group):** (n=5) rats were given I.P. injection of LPS (3mg/kg. B.W)<sup>[15]</sup>.

**Group III (LF-treated group):** (n=5) rats were given LPS as in group II. One hour later rats were given I.P. injection of LF (5mg/rat).

**Group IV (DEXA-treated group):** (n=5) rats were given LPS as in group II. One hour later rats were given IP injection of DEXA (5mg/kg. B.W).

#### *Sample collection and preparation of tissue*

All animals were sacrificed 24 hours after the last injection. Rats were sacrificed after ether inhalation anesthesia and both lungs were dissected from the thoracic cage. The bodies of the dead animals were disposed of by incinerator.

The right lung was processed for histological examination and the left lung for immunohistochemical examination. The lungs were fixed in 10% formalin solution for one week followed by dehydration using ascending grades of ethyl alcohol, then the tissues were cleared with xylene, impregnated in soft paraffin at 56°C followed by embedding in paraffin blocks. Serial sections were cut at 4-5 µm thickness and were processed to the following techniques: Hematoxylin and eosin stain (H&E), orcein stain for elastic fibers, Periodic acid Schiff's reaction (PAS) for goblet cells, and toluidine blue stain for mast cells.

The paraffin blocks of the left lungs were cut on positively charged slides and were processed for immunohistochemical reaction using (iNOS) antibodies. Inducible NOS is expressed in response to proinflammatory factors and cytokines. iNOS antibody (rabbit polyclonal, cat# Epredia RB-1605-P1ABX, code: 12623077; at dilution of 1/100) was obtained from Lab Vision, Thermo Fisher Scientific, Fremont, CA, USA. Sections were counterstained with Mayer's hematoxylin. The positive control was rat lung, Negative control sections were processed by the same protocol except for the primary antibody which was replaced by PBS. Positive immune reactions for iNOS appeared as brown cytoplasmic dots or granules<sup>[18]</sup>.

#### *Histomorphometric Study*

The histomorphometric study was performed by the image analyzer at the Histology Department, Faculty of Medicine, Ain Shams University using Leica QW in V.3 image analysis software (Leica Microsystems, Wetzlar, Germany) installed on a Dell Personal Computer (PC) (Texas, USA). The PC was connected to a microscope

(Leica microsystem, Heerburg, Switzerland). All groups were subjected to the morphometric study. All measurements were obtained from 5 different fields from each section. Five sections from 5 different animals of each group and subgroup to measure the mean of the following:

1. The thickness of the interalveolar septum in  $\mu\text{m}$ : The wall between two adjacent alveolar lumens (x 20).
2. The alveolar space surface area percentage: The alveolar space surface area percentage was measured using (x 20).
3. The number of goblet cells in PAS-stained sections (x 40).
4. The number of mast cells in toluidine blue stained sections (x 20).
5. The area percentage of iNOS-positive cells in immunohistochemically stained sections (x 40).

### **Statistical analysis**

The measured parameters by the image analyzer were statistically analyzed using SPSS program version 20, IBM Corporation. The mean value and the standard deviation (SD) were calculated in different groups. Data were evaluated using One-way analysis of variance test (ANOVA) to compare between means. Values were presented as mean  $\pm$  (SD). The least significant difference (LSD) post-hoc test was done to detect significance between groups. The significance of data was determined by the *P* value:  $P > 0.05$  was considered non-significant, and  $P \leq 0.05$  was considered significant.

## **RESULTS**

---

### **General observation**

In the control group, all rats appeared in good general condition, with normal moving activities in the cages, normal sniffing, and digging the sawdust. The extracted lungs from all subgroups were pink in color and appeared homogenous. On the other hand, in the lipopolysaccharide (ALI) group (Group II), the rats were noticed with lower energetic activity than the control group. The extracted lungs appeared mildly increased in size in comparison to the control group. The rats in the lactoferrin group (Group III) showed apparently better activities than group II. Also, the rats in the dexamethasone group (Group IV) showed apparently better activities than groups II and III. Moreover, the extracted lungs of group III and group IV appeared comparable to those of the control group. All rats of all groups remained alive throughout the experiment.

### **Histological and histomorphometric results**

The control animals of subgroups 1B, 1C, and 1D (data not shown) showed similar histological findings as the control subgroup 1A in all histological techniques.

### **The H&E-stained sections**

Examination of the H&E-stained sections of the lungs of the control subgroups demonstrated a sponge-like appearance. The lungs consisted of terminal bronchioles of variable sizes, numerous patent alveoli, alveolar sacs, and alveolar ducts. The terminal bronchioles were lined by simple columnar epithelium with Clara cells (club cells) having dome-shaped apices. Alveoli opening in respiratory bronchioles which were lined by cuboidal epithelium were detected. Alveoli and alveolar sacs were lined by Type I and type II pneumocytes. Type I pneumocytes appeared flat with flattened nuclei. Type II pneumocytes were seen as scattered cuboidal cells with rounded nuclei, foamy cytoplasm, and bulging into the alveolar lumen. Thin interalveolar septa were seen between the alveolar spaces consisting of a thin layer of connective tissue with many small blood capillaries (Figures 1A-C). Examination of the H&E-stained sections of the lipopolysaccharide-treated group showed marked focal structural changes in the lung. Some areas appeared more greatly affected than others. The most prominent findings were the massive infiltration of mononuclear cells around the bronchioles, blood vessels, and in the IAS and in alveoli. In certain areas, the mononuclear cellular infiltration could be seen in the lumen of alveoli. Most mononuclear cells were neutrophils, eosinophils, and macrophages. Neutrophils were identified by their segmented nuclei, eosinophils by their characteristic acidophilic cytoplasm and bilobed nuclei, and macrophages by their large size and basophilic cytoplasm. The epithelium of most bronchioles appeared occasionally desquamated and shed in the lumen. Most alveoli showed an apparent narrowing of the alveolar space with total collapse in certain areas. Some regenerated alveoli were lined by cuboidal cells most probably pneumocytes type II. The IAS showed numerous capillaries (Figures 1D- H).

Examination of the H&E-stained sections of the lactoferrin-treated group showed the structure of the lung nearly similar to the control group. All changes were apparently less when compared to group II. Most of the interalveolar septa appeared thin compared to group II with most of the alveoli being patent. Nevertheless, mild thickened interalveolar septa were noticed. Mild mononuclear cellular aggregation was detected around some bronchioles. Most bronchioles showed intact epithelium, however, some exfoliation of the lining epithelium was detected in a few bronchioles. The alveoli were lined by type I and type II pneumocytes. There was an apparent mild increased number of type II pneumocytes compared to the control group but apparently less than group II. The blood vessels appeared similar to those of the control group with very few leukocytes infiltrating the wall (Figures 1I,J).

Examination of the H&E-stained sections of the dexamethasone-treated group showed that the structure of the lung was very similar to the control group. Most of the interalveolar septa appeared thin compared to group

II and most of the alveoli appeared patent. Nevertheless, minimal thickening in the wall of the interalveolar septa was noticed. Minimal mononuclear cellular aggregation was detected around some bronchioles. Most bronchioles showed intact regular epithelium with less desquamated epithelium in the lumen. Type I and type II pneumocytes lined the alveoli. The blood vessels appeared similar to the control group (Figures 1K).

These findings were confirmed with morphometric and statistical analysis. A significant decrease in the mean surface area percentage of the alveolar spaces and a significant increase in the mean thickness of the interalveolar septa (IAS) of the LPS and LF groups were noticed compared to the control subgroup IA. In the LF and DEXA groups, there was a significant increase in the mean surface area percentage of the alveolar spaces and a significant decrease in the mean thickness of the IAS compared to the LPS group. However, a non-significant decrease in the mean surface area percentage of the alveolar spaces and a significant increase in the mean thickness of the IAS was noticed between DEXA and the control subgroup IA. (Table 1)

#### ***Toluidine blue-stained sections of the lung***

Examination of toluidine blue of the lung sections of the control subgroups showed an apparently few mast cells in the interalveolar septa (Figure 2A). Sections of the LPS group showed an apparent increase in the number of metachromatically stained mast cells in the interalveolar septa. (Figure 2B). After treatment with LF (group III) the lung tissues showed few metachromatically stained mast cells in the wall of the bronchiole and the interalveolar septa (Figure 2C). Apparent few metachromatically stained mast cells were detected in the interalveolar septa in the DEXA group (Figure 2D). In the LPS and LF groups, a significant increase in the mean number of mast cells was noticed compared to the control subgroup IA. A significant decrease in the LF and DEXA groups was noticed compared to group LPS group. However, there was a non-significant change in the mean number of mast cells between the control subgroup IA, LF, and DEXA groups (Table 1)

#### ***PAS-stained sections of the lung***

The control subgroups showed few scattered PAS-positive goblet cells in the lining epithelium of the bronchial passages (Figure 3A). While the LPS group showed an apparent increase in the number of goblet cells in the lining epithelium of bronchioles compared

to the control group (Figure 3B). After treatment with lactoferrin and DEXA, the lungs showed an apparent decrease in the number of PAS-positive goblet cells in the lining epithelium of bronchioles as compared to group II (Figures 3C, D) respectively. In the LPS and LF groups, a significant increase in the mean number of PAS-positive goblet cells was detected compared to the control subgroup IA. A significant decrease in the mean number of PAS-positive goblet cells was noticed in LF and DEXA groups compared to group II. Moreover, a significant decrease in the mean number in the DEXA group was noticed compared to the LF group (Table 1).

#### ***Orcein-stained sections of the lung***

The control subgroups showed prominent elastic fibers in the wall of bronchioles, blood vessels, and alveoli (Figure 4A). With LPS the lung tissues showed an apparent decrease in the elastic fiber content compared to the control group. Elastic fibers appeared discontinuous around the wall of the bronchioles, and alveoli. However, the elastic fibers around blood vessels were not affected. (Figure 4B). After treatment with LF and DEXA the lung tissues showed elastic fibers in the wall of bronchioles, alveoli, and blood vessels similar to the control group. In the DEXA group, the elastic fibers were apparently not affected (Figures 4C,D) respectively.

#### ***The immunohistochemical staining for induced nitric oxide synthase (iNOS)***

The control subgroup showed weak positive cytoplasmic immunoreaction in the epithelium of the alveoli and bronchioles. (Figures 5A,B). In the LPS-treated group, the sections showed a strong positive immune reaction to iNOS antibodies compared to the control group. This was detected in the cytoplasm of cells lining the alveoli, cells in the interalveolar septa, and those lining the bronchioles (Figures 5C,D). The sections treated with LF showed moderate positive immunoreactions to iNOS in the cytoplasm of the cells lining the bronchioles, and alveolar epithelium compared to group II (Figures 5E,F). In the DEXA-treated group, there was a weak positive immune reaction to iNOS in the epithelial lining of bronchioles, and alveolar epithelium compared to groups II and III (Figures 5G, H). A significant increase in the mean area percentage of iNOS-positive cells in LPS and LF-treated groups compared to the control group. A significant decrease was detected in the LF and DEXA groups compared to the LPS group. However, there was a non-significant change in the mean area percentage of iNOS-positive cell between the control subgroup IA, LF, and DEXA groups (Table 1).

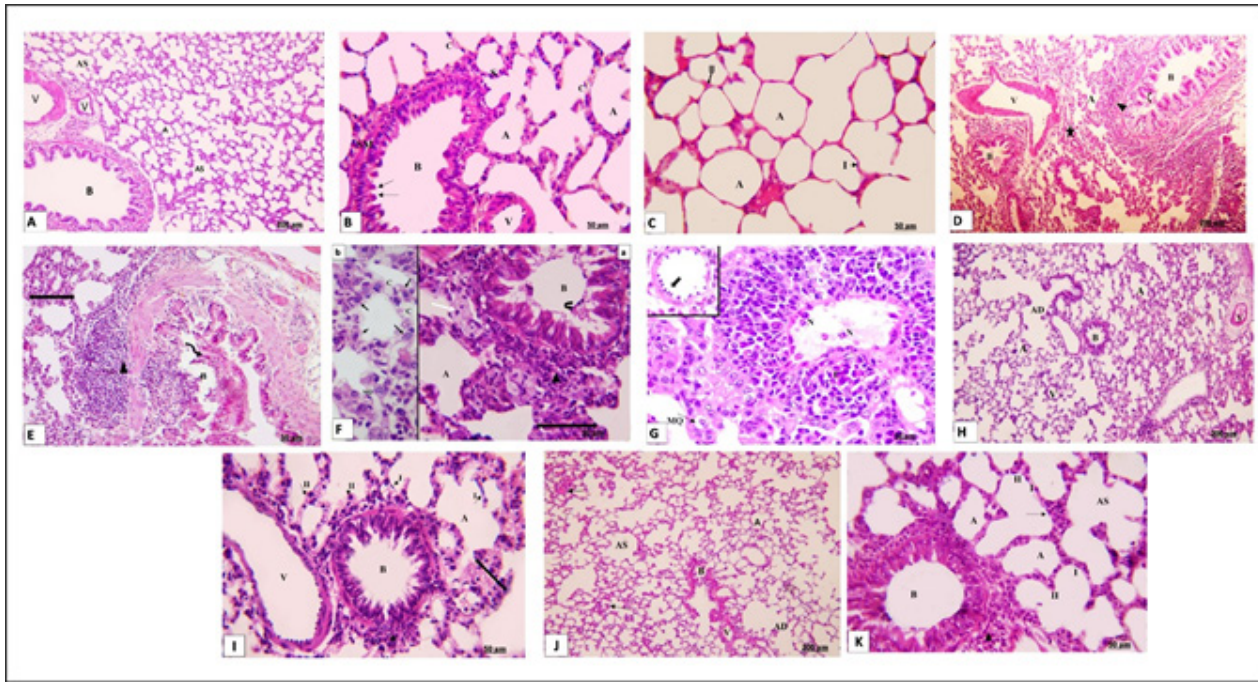


**Fig. 1:** Photomicrographs of H&E-stained lung sections from different groups. [A, B, C] control subgroup IA: bronchiole (B); dome-shaped club cells ( $\uparrow$ ); smooth muscle fibers (SM) in the bronchiolar wall; Lung alveoli (A), alveolar sacs (AS), blood vessels (V), flat type I pneumocytes (I), cubical type II pneumocytes with round nuclei (II), interalveolar septa (S), capillaries (C). [D, E, F, G] LPS (ALI) group: [D, E, F(a,b)]: bronchiole (B), mononuclear cells infiltrating the wall ( $\blacktriangle$ ); separation and desquamation of bronchiolar epithelium (curved arrow), narrow alveoli (A) collapsed alveolar areas (\*), thickened interalveolar septa ( $\downarrow$ ), macrophages (MQ), type II pneumocytes ( $\uparrow$ ), dilated capillaries (C), neutrophils (N), eosinophils (E). (F): Notice the presence of submucosal glands (white arrow). [G] mononuclear cellular infiltration surrounding the alveolar lumen and the inflammatory cells aggregating in the interalveolar septum; neutrophils (N), foamy macrophages (MQ), and eosinophils (E). Inset: regenerated alveoli lined by type II pneumocytes ( $\uparrow$ ). [H, I] LF-treated group: normal bronchiole (B), cellular infiltration (\*), thickening of interalveolar septa ( $\downarrow$ ), alveolar duct (AD), patent alveoli (A), thin wall blood vessel (V), type I pneumocytes (I $\uparrow$ ), type II pneumocytes (II $\uparrow$ ). [J, K] DEXA treated group: bronchiole (B), patent alveoli (A), alveolar sacs (AS), blood vessel (V), alveolar ducts (AD), inflammatory cells ( $\blacktriangle$ ), type I (I) and type II (II) pneumocytes, mildly thickened interalveolar septa ( $\uparrow$ ). [A, D, H, J  $\times$  100, scale bar: 200  $\mu$ m] [B, C, E, F, G, I, K  $\times$  400, scale bar: 50  $\mu$ m]

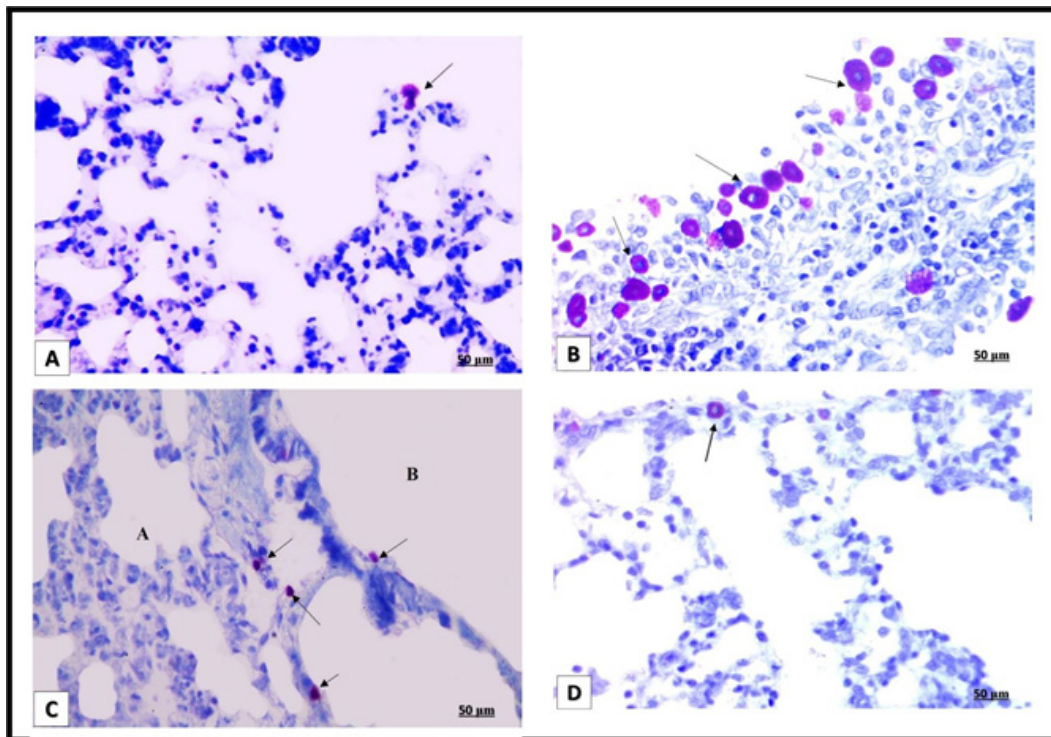


**Fig. 2:** Photomicrographs of toluidine blue stain in lung sections from different groups  $\times$ 400, (scale bar: 50  $\mu$ m). [A] control subgroup IA showing one mast cell in interalveolar septa ( $\uparrow$ ). [B] The LPS-(ALI) group showing an apparent increase in the number of metachromatically stained mast cells in the interalveolar septa ( $\uparrow$ ). [C, D] The LF and DEXA-treated groups respectively showing an apparent few mast cells in the wall of bronchiole (B) and interalveolar septa ( $\uparrow$ ).

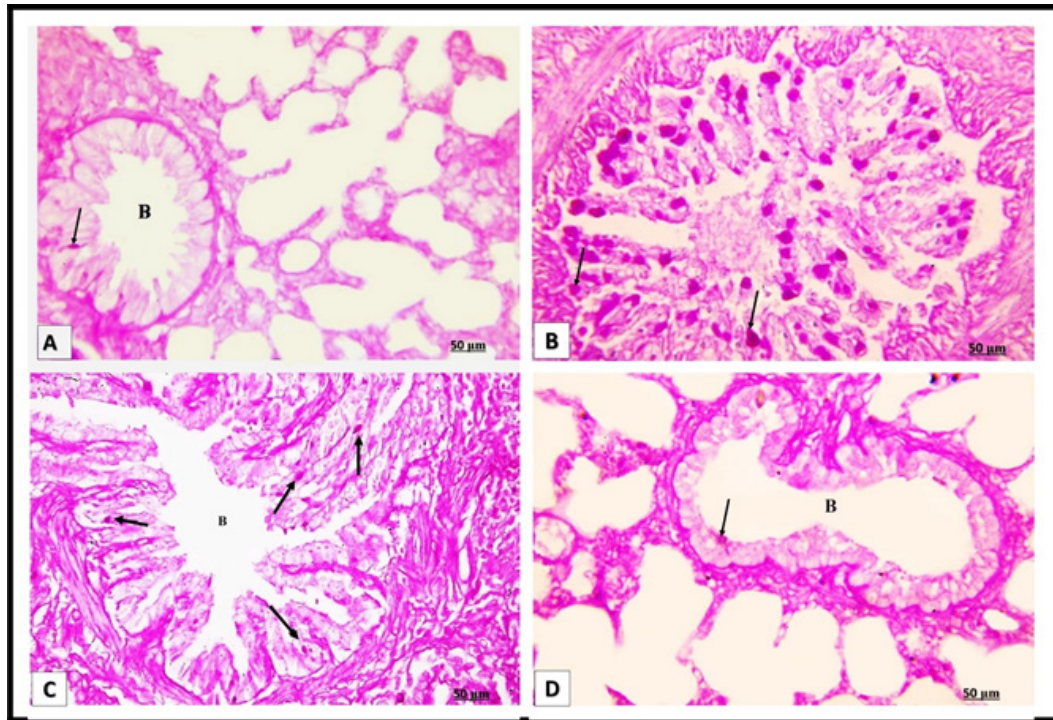


**Fig. 3:** Photomicrographs of PAS stain in lung sections from different groups  $\times 400$ , (scale bar: 50  $\mu\text{m}$ ). [A] Control subgroup IA: showing few PAS-positive goblet cells ( $\uparrow$ ) in the lining epithelium of a bronchiole (B). [B] The LPS-treated group showing an increase in PAS-positive goblet cells ( $\uparrow$ ) in the lining epithelium of the bronchiole. [C, D] The LF and DEXA-treated groups respectively: few PAS-positive goblet cells ( $\uparrow$ ) in the lining epithelium of the bronchiole (B).

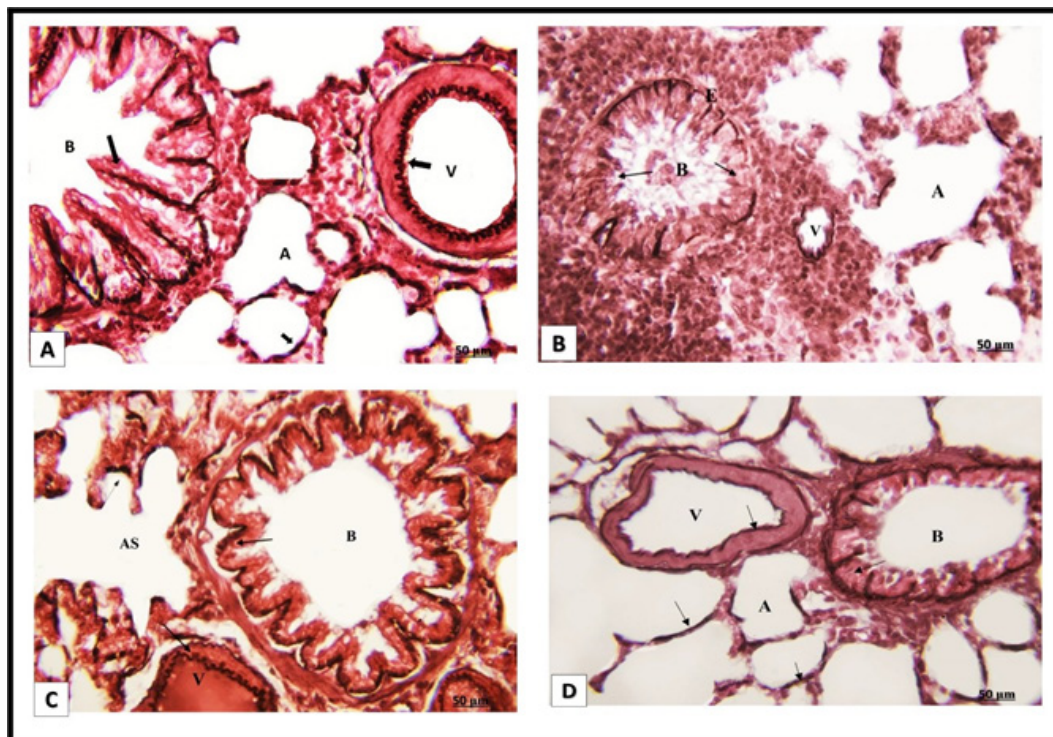


**Fig. 4:** Photomicrographs of orcein stain in lung sections from different groups  $\times 400$ , (scale bar: 50  $\mu\text{m}$ ). [A] control subgroup IA showing elastic fibers ( $\uparrow$ ) in the wall of a bronchiole (B), alveoli (A), and blood vessel (V). [B] The LPS-treated group showing discontinuous elastic fibers ( $\uparrow$ ) in the wall of a bronchiole (B) and alveoli (A) blood vessel (V). [C, D] The LF and DEXA-treated groups respectively showing prominent elastic fibers ( $\uparrow$ ) in the wall of a bronchiole (B), alveolar sac (AS), and blood vessel (V).

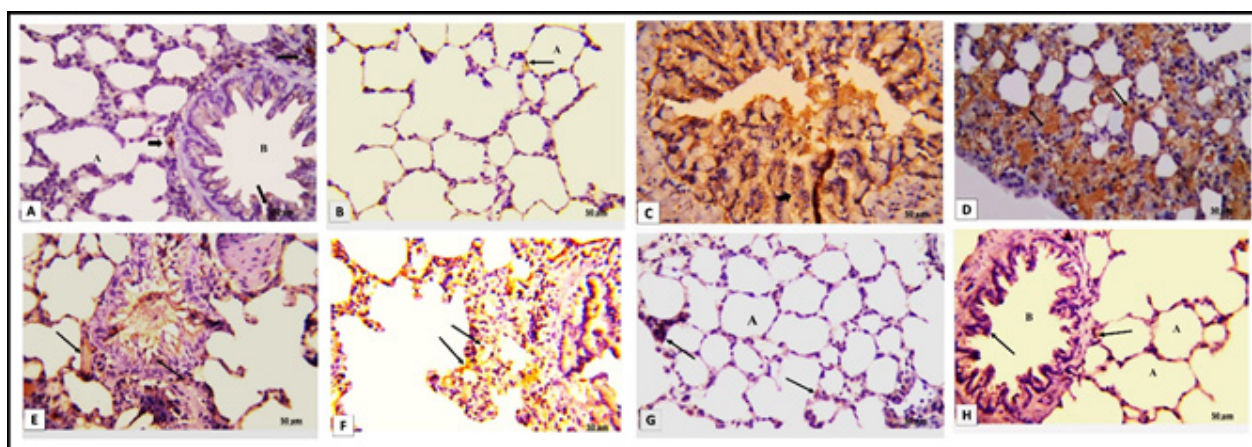


**Fig. 5:** Photomicrographs of iNOS immunoreaction in lung sections from different groups  $\times 400$ , (scale bar: 50  $\mu\text{m}$ ). [A, B] control subgroup IA showing a weak positive iNOS immunoreaction (arrow) in the epithelium of alveoli (A) and bronchiole (B). [C,D] The LPS-treated group showing strong cytoplasmic positive iNOS immunoreactions ( $\uparrow$ ) in the cells lining the alveoli and in the epithelium of the bronchiole. [E,F] The LF-treated groups showing an apparent moderate positive cytoplasmic iNOS immune reaction ( $\uparrow$ ) in cells of alveolar epithelium and in the epithelium of bronchiole. [G,H] DEXA treated group showing a weak positive cytoplasmic iNOS immune reaction ( $\uparrow$ ) in the alveolar epithelium (A) and in the epithelium lining of a bronchiole (B).

**Table 1:** The effect of LPS, LF, and DEXA on the mean of the alveolar space surface areas, thickness of the interalveolar septum, mean number of PAS-positive goblet cells, mean number of mast cells and mean area percentage of iNOS positive cells in different groups

The mean value	Control subgroup IA	LPS	LPS+LF	LPS+DEXA
The mean alveolar space surface area percentage	64.20 ( $\pm$ 8.8)	33.46 ( $\pm$ 6.6)*	56.17 ( $\pm$ 8.1)*#	61.16 ( $\pm$ 4.1)#
The Mean thickness of interalveolar septa	6.2 ( $\pm$ 0.64)	14.1 ( $\pm$ 0.86)*	9.2 ( $\pm$ 1.27)*#	7.9 ( $\pm$ 1.18)*#•
The Mean number of PAS-positive goblet cells	3.2 ( $\pm$ 0.8)	31.6 ( $\pm$ 5.6)*	11.2 ( $\pm$ 2.9)*#	5.4 ( $\pm$ 1.2)*#
Mean number of mast cells	2.3 ( $\pm$ 0.94)	11.5 ( $\pm$ 2.04)*	3.6 ( $\pm$ 1.04)*#	2.8 ( $\pm$ 0.80)#
Mean area percentage of iNoS positive cells	0.1% ( $\pm$ 0.03)	1.7% ( $\pm$ 0.59)*	0.4% ( $\pm$ 0.89)*#	0.3% ( $\pm$ 0.81)#

Data are mean  $\pm$  SD of 5 rats per group. \* $P < 0.05$ , vs. control subgroup IA; # $P < 0.05$ , vs LPS group, •  $P < 0.05$ , vs LPS+LF group, LPS: lipopolysaccharide, LF: lactoferrin, DEXA: dexamethasone by One-way ANOVA with Tukey post hoc test.

## DISCUSSION

Acute lung injury is a major cause of respiratory failure disease. It affects the lung structure by producing severe lung inflammation and alveolar damage and has a high mortality rate<sup>[3]</sup>.

This study was designed to assess the therapeutic use of LF versus DEXA on the structure of the lung in a model of LPS-induced acute lung injury.

LPS is a well-established model for the investigation of ALI as it mimics acute lung inflammation and the associated histological findings in the lung<sup>[19]</sup>. The mechanisms by which LPS causes lung injury include increased production of reactive oxygen species, inflammatory cell activation, and cytokines release which are similar to those occurring in cases of ARDS<sup>[20]</sup>.

In the present study, light microscopic examination of lung specimens from rats injected with LPS showed manifest focal affection of lung structure. large areas of mononuclear cellular infiltrations were detected in many sections with numerous neutrophils, eosinophils, and macrophages and shedding of the epithelium. The increased infiltration of mononuclear cells detected subsequently led to the narrowing of the alveolar spaces.

These findings agreed with Hsieh *et al.*<sup>[21]</sup> and Zeng *et al.*<sup>[22]</sup> they explained that the filtration of the activated inflammatory cells in the alveolar wall leads to the release of inflammatory cytokines like tumor necrosis factor- $\alpha$  (TNF- $\alpha$ ), IL-1 $\beta$ , iNOS from airway epithelium and activation of reactive oxygen species and oxidative stress. Another mechanism was described by Ciesielska *et al.*<sup>[23]</sup>, where LPS induced inflammation through the activation of nuclear factor- $\kappa$ B (NF- $\kappa$ B) and increased the expression of inflammatory cytokines such as IL-1 $\beta$ , IL6, and TNF- $\alpha$  to modulate inflammatory reactions. These inflammatory cytokines lead to the shedding of epithelium and pulmonary edema.

lipopolysaccharides increased the degradation of the epithelium glycocalyx and destroyed tight junction proteins: occludin, and claudin 4, leading to an increase in the permeability of the alveolar barrier and exudation of inflammatory cells. Also, LPS disrupts the endothelial barrier which increases the infiltration of blood proteins, toxic substances, and immune cells into the vessel wall<sup>[24]</sup>.

Damage of alveolar epithelium by LPS led to an apparent increase in type II pneumocytes. Type II pneumocytes are considered stem cells that underwent proliferation in an attempt to repair the degenerated epithelium<sup>[25]</sup>.

In the present study, the foamy macrophages were observed in the sections of the lung that were exposed to LPS. Macrophages can be divided into two types; classically activated phenotype (M1) which is linked to pro-inflammatory responses, and the alternatively activated phenotype (M2) which plays a key role in anti-inflammatory reactions<sup>[26]</sup>. Injury to pneumocytes II led to the release of stored lipids in extracellular space to be taken by macrophages. The presence of oxidized lipids inside macrophages led to changes in the gene expression of macrophages (M2) that help the process of repair by suppressing the immune response in the lung<sup>[27]</sup>. Neutrophils can stimulate the proliferation of type II pneumocytes. The neutrophils don't elicit inflammation only, but also share in initiating the repair<sup>[28]</sup>.

A significant increase in the number of mast cells was noticed in the current study with LPS compared to the control group. LPS was able to aggravate an existing inflammatory state in allergic airway inflammation via T helper cell 2 cytokine production<sup>[29]</sup>. Mast cell proteases play critical roles in the recruitment of both neutrophils and eosinophils to sites of inflammation<sup>[30]</sup>. This could explain increased neutrophils and eosinophils in the LPS group of the present study. Similarly, the release of histamine from mast cells enhances adhesion molecule expression, and P-selectin upregulation which mediates neutrophil adhesion and recruitment<sup>[31]</sup>.

The LPS group in the present study showed a significant increase in the number of PAS-positive goblet cells compared to the control group. Similarly, it was reported that LPS resulted in goblet cell proliferation and hyperplasia<sup>[32]</sup>. LPS-induced mucin secretion in goblet cells could occur through the LPS-dependent pathway or IL-8-dependent pathway, or both pathways<sup>[33]</sup>.

Submucosal glands were detected in the present study in the wall of the bronchioles in the LPS-treated group, these findings go with Yanagihara *et al.* who proved that LPS induces mucous cell metaplasia in mouse lungs<sup>[34]</sup>.

Lipopolysaccharides cause an apparent decrease in the amount of elastic fibers in the lung which leads to decreased lung tissue resistance, as elastic fibers regulate tissue resistance and elastance. These findings agreed with Monção-Ribeiro *et al.*<sup>[35]</sup>. Lipopolysaccharides cause ARDS which leads to a decrease in lung compliance and an increase in lung resistance and pulmonary edema<sup>[36]</sup>.

In the present study, LPS induced the expression of iNOS in the inflammatory cells in the IAS and in the bronchial epithelium. The expression occurred in various pulmonary cell types such as macrophages, neutrophils, bronchial epithelium, and pulmonary artery smooth muscle cells<sup>[37]</sup>. Lipopolysaccharides increase the secretion of cytokines from macrophages and neutrophils which are known as an important source of expression of the high level of iNOS leading to more increase in the expression of NO<sup>[38]</sup>.

In the present study, the microscopic examination of lung sections of rats injected intraperitoneally by LPS and Lactoferrin showed improvement with mild affection of the structure of the lung. These findings were confirmed with histological and morphometric analysis. These agreed with Li *et al.*,<sup>[39]</sup> who referred the improvement to the anti-inflammatory, antioxidant properties and the protective role of LF against various microbial infections.

Many authors suggested the action of LF to reduce LPS-induced lung inflammation, Gupta *et al.*<sup>[40]</sup> suggested that the bactericidal activity of LF was through the destruction of the gram-negative bacteria outer membrane and the immunoregulator effect by enhancing the cytotoxicity of natural killer cells and monocytes and decreasing the release of TNF $\alpha$ , IL-1, and IL-2. Lactoferrin inhibits the LPS action by binding with CD14 on monocytes and macrophages<sup>[41]</sup>. They added that LF acted as LPS binding protein which had a high affinity and competed with other binding proteins, therefore it interfered with the action of LPS.

The biological activities of LF were through its binding with membrane receptors as CD14, TLR2, TLR4, intelectin-1, and cytokine receptor 4<sup>[3]</sup>. Or through regulation of the NF $\kappa$ B/MAPK pathway, decreased the release of reactive oxygen species, and maintained barrier integrity<sup>[42]</sup>.

Lu *et al.*,<sup>[43]</sup> explained the antibacterial activity of LF towards different bacterial pathogens to be through the sequestration of iron, targeting bacterial virulence mechanisms, destabilization of the membrane, and invasion of host cells and proved that LF can decrease the level of nitric oxide and TNF- $\alpha$  as well as decreasing iNOS.

In the present study, the microscopic examination, and the morphometric and statistical analysis of the lung tissues of rats injected intraperitoneally by LPS and DEXA showed that the structure of the lung was very similar to the control group with minimal affection on the lung tissue. It was reported that dexamethasone decreased lung inflammation in the lung injury induced by LPS by regulating the expression of the TLR-4 pathway and decreased lung myeloperoxidase<sup>[44]</sup>. Dexamethasone appeared to have an inhibitory effect on leakage in the microvasculature. This effect is thought to diminish the cellular sources of proinflammatory and vasoactive mediators, and possibly by a direct inhibited permeability effect on the microvasculature. This led to reduced pulmonary edema and improved histological changes<sup>[45]</sup>.

In the present study, DEXA decreased mucus secretion, goblet cells in the airways of LPS-induced acute lung injury, prevented collagen increment, inhibited elastic fragmentation, and caused minimal positive immune reaction to iNOS antibodies-stained sections these findings agreed with the authors<sup>[46,47,48]</sup>.

Cytokine-stimulated inducible nitric oxide synthase (iNOS) gene expression is dependent on NF- $\kappa$ B activation

and is suppressed by dexamethasone. Meanwhile, dexamethasone markedly suppressed iNOS mRNA and protein expression<sup>[42]</sup>.

## CONCLUSION

---

LPS injection resulted in marked changes in lung structure which mimicked acute lung injury. Administration of lactoferrin or dexamethasone at the time of acute lung injury had a protective, ameliorative, and therapeutic effect on the lung through the anti-inflammatory and antioxidant effects of both. The therapeutic effects of dexamethasone were more prominent than lactoferrin.

## FUNDING RESOURCES

---

This research did not receive any specific grant from funding agencies in the public, commercial, or not-for-profit sectors.

## CONFLICT OF INTERESTS

---

There are no conflicts of interest.

## REFERENCES

---

1. Bellani, G., Laffey, J. G., Pham, T., Fan, E., Brochard, L., Esteban, A., *et al.* Epidemiology, patterns of care, and mortality for patients with acute respiratory distress syndrome in intensive care units in 50 countries.. *JAMA*. 2016, 315, 788–800. doi:10.1001/jama.2016.0291
  2. Domscheit H, Hegeman MA, Carvalho N, Spieth PM. Molecular Dynamics of Lipopolysaccharide-Induced Lung Injury in Rodents. *Front Physiol*. 2020 Feb 5; 11:36. DOI: 10.3389/fphys.2020.00036
  3. Kell DB, Heyden EL, Pretorius E. The Biology of Lactoferrin, an Iron-Binding Protein That Can Help Defend Against Viruses and Bacteria. *Front Immunol*. 2020; 11:1221. DOI: 10.3389/fimmu.2020.01221
  4. Mokrá D. Acute lung injury - from pathophysiology to treatment. *Physiol Res*. 2020 Dec 31;69(Suppl 3):S353-S366. DOI: 10.33549/physiolres.934602
  5. Farhana A, Khan YS. Biochemistry, lipopolysaccharide. InStatPearls [Internet] 2022 Apr 21. StatPearls Publishing. PMID: 32119301 Bookshelf ID: NBK554414
  6. Wei M, Chu X, Jiang L, Yang X, Cai Q, Zheng C, Ci X, Guan M, Liu J, Deng X. Protocatechuic acid attenuates lipopolysaccharide-induced acute lung injury. *Inflammation*. 2012 Jun;35(3):1169-78.DOI: 10.1007/s10753-011-9425-2
  7. Yao, X., Bunt, C., Cornish, J., Quek, S. Y., & Wen, J. Improved RP-HPLC method for determination of bovine lactoferrin and its proteolytic degradation in simulated gastrointestinal fluids. (2013). *Biomedical Chromatography*, 27(2), 197-202. DOI: 10.1002/bmc.2771
  8. Chang, R.; Zen Sun, W.; Bun Ng, T. Lactoferrin as potential preventative and treatment for COVID-19. *Authorea* 2020. DOI: 10.1016/j.ijantimicag.2020.106118
  9. Bolat E, Eker F, Kaplan M, Duman H, Arslan A, Saritaş S, Şahutoğlu AS, Karav S. Lactoferrin for COVID-19 prevention, treatment, and recovery. *Front Nutr*. 2022; 9:992733.doi: 10.3389/fnut.2022.992733
  10. Gao W, Tong D, Li Q, Huang P and Zhang F: Dexamethasone promotes regeneration of crushed inferior alveolar nerve by inhibiting NF-κB activation in adult rats. *Arch Oral Biol*. 80:101–109. 2017.DOI: 10.1016/j.archoralbio.2017.03.025
  11. Koliaş AG, Edlmann E, Thelin EP, Bulters D, Holton P, Suttner N, Owusu-Agyemang K, Al-Tamimi YZ, Gatt D, Thomson S, Anderson IA, Richards O, Whitfield P, Gherle M, Caldwell K, Davis-Wilkie C, Tarantino S, Barton G, Marcus HJ, Chari A, Brennan P, Belli A, Bond S, Turner C, Whitehead L, Wilkinson I, Hutchinson PJ. British Neurosurgical Trainee Research Collaborative (BNTRC) and Dex-CSDH Trial Collaborators. Dexamethasone for adult patients with a symptomatic chronic subdural haematoma (Dex-CSDH) trial: study protocol for a randomised controlled trial. *Trials*. 2018; 19(1):670. doi: 10.1186/s13063-018-3050-4.
  12. Crane BR, Sudhamsu J, Patel BA. Bacterial nitric oxide synthases. *Annu Rev Biochem*. 2010; 79:445-470. DOI: 10.1146/annurev-biochem-062608-103436
  13. Pradhan AA, Bertels Z, Akerman S. Targeted Nitric Oxide Synthase Inhibitors for Migraine. *Neurotherapeutics*. 2018; 15(2):391-401.DOI: 10.1007/s13311-018-0614-7
  14. Cinelli MA, Do HT, Miley GP, Silverman RB. Inducible nitric oxide synthase: Regulation, structure, and inhibition. *Med Res Rev*. 2020; 40(1):158-189. DOI: 10.1002/med.21599
  15. Li W, Wu F, Chen L, Li Q, Ma J, Li M, Shi Y. Carbon Monoxide Attenuates Lipopolysaccharides (LPS)-Induced Acute Lung Injury in Neonatal Rats via Downregulation of Cx43 to Reduce Necroptosis. *Med Sci Monit*. 2019; 25:6255-6263. DOI: 10.12659/MSM.917751
  16. Li W, Fu K, Lv X, Wang Y, Wang J, Li H, Tian W, Cao R. Lactoferrin suppresses lipopolysaccharide-induced endometritis in mice via down-regulation of the NF-κB pathway. *Int Immunopharmacol*. 2015; 28(1):695-699. doi: 10.1016/j.intimp.2015.07.040.
  17. Yang JW, Mao B, Tao RJ, Fan LC, Lu HW, Ge BX, Xu JF. Corticosteroids alleviate lipopolysaccharide-induced inflammation and lung injury via inhibiting NLRP3-inflammasome activation. *J Cell Mol Med*. 2020; 24(21):12716-12725. DOI: 10.1111/jcmm.15849
-

18. Elsyade RH, Sadek DR. The Possible Ameliorative Effect of Naringenin versus Flaxseed Oil on Renal Lead Toxicity in Male Albino Rats: A Histological and Immunohistochemical Study. *Journal of Microscopy and Ultrastructure*. 2023 Nov 2. DOI: 10.4103/jmau.jmau\_61\_23
19. Kolomaznik M, Nova Z, Calkovska A. Pulmonary surfactant and bacterial lipopolysaccharide: the interaction and its functional consequences. *Physiol Res*. 2017; 66:S147–S157. DOI: 10.33549/physiolres.933672
20. Dong Z, Yuan Y. Accelerated inflammation and oxidative stress induced by LPS in acute lung injury: Inhibition by ST1926. *Int J Mol Med*. 2018; 41(6):3405-3421. DOI: 10.3892/ijmm.2018.3574
21. Hsieh YH, Deng JS, Pan HP, Liao JC, Huang SS, Huang GJ. Sclareol ameliorate lipopolysaccharide-induced acute lung injury through inhibition of MAPK and induction of HO-1 signalling. *Int Immunopharmacol*. 2017; 44:16–25. doi: 10.1016/j.intimp.2016.12.026.
22. Zeng M, Sang W, Chen S, Chen R, Zhang H, Xue F, Li Z, Liu Y, Gong Y, Zhang H, Kong X. 4-PBA inhibits LPS-induced inflammation through regulating ER stress and autophagy in acute lung injury models. *Toxicol Lett*. 2017; 271:26-37. doi: 10.1016/j.toxlet.2017.02.023.
23. Ciesielska A, Matyjek M, Kwiatkowska K. TLR4 and CD14 trafficking and its influence on LPS-induced pro-inflammatory signaling. *Cell Mol Life Sci*. 2021; 78(4):1233-1261. DOI: 10.1007/s00018-020-03656-y
24. Li HY, Yang HG, Wu HM, Yao QQ, Zhang ZY, Meng QS, Fan LL, Wang JQ, Zheng N. Inhibitory effects of lactoferrin on pulmonary inflammatory processes induced by lipopolysaccharide by modulating the TLR4-related pathway. *J Dairy Sci*. 2021; 104(7):7383-7392. DOI: 10.3168/jds.2020-19232
25. Olajuyin AM, Zhang X, Ji HL. Alveolar type 2 progenitor cells for lung injury repair. *Cell death discovery*. 2019 Feb 8;5(1):63. doi.org/10.1038/s41420-019-0147-9.
26. Cheng P, Li S, Chen H. Macrophages in Lung Injury, Repair, and Fibrosis. *Cells*. 2021 Feb 18;10(2):436. doi: 10.3390/cells10020436.
27. Gower WA, Noguee LM. Surfactant dysfunction. *Paediatr Respir Rev*. 2011 Dec;12(4):223-9. doi: 10.1016/j.prrv.2011.01.005.
28. Paris AJ, Liu Y, Mei J, Dai N, Guo L, Spruce LA, Hudock KM, Brenner JS, Zacharias WJ, Mei HD, Slamowitz AR, Bhamidipati K, Beers MF, Seeholzer SH, Morrisey EE, Worthen GS. Neutrophils promote alveolar epithelial regeneration by enhancing type II pneumocyte proliferation in a model of acid-induced acute lung injury. *Am J Physiol Lung Cell Mol Physiol*. 2016 Dec 1;311(6):L1062-L1075. doi: 10.1152/ajplung.00327.2016.
29. Cho KA, Park M, Kim YH, Choo HP, Lee KH. Benzoxazole derivatives suppress lipopolysaccharide-induced mast cell activation. *Mol Med Rep*. 2018 May;17(5):6723-6730. DOI: 10.3892/mmr.2018.8719
30. Dudeck J, Kotrba J, Immler R, Hoffmann A, Voss M, Alexaki VI, Morton L, Jahn SR, Katsoulis-Dimitriou K, Winzer S, Kollias G, Fischer T, Nedospasov SA, Dunay IR, Chavakis T, Müller AJ, Schraven B, Sperandio M, Dudeck A. Directional mast cell degranulation of tumor necrosis factor into blood vessels primes neutrophil extravasation. *Immunity*. 2021 Mar 9;54(3):468-483.e5. doi: 10.1016/j.immuni.2020.12.017.
31. Zhang J, Alcaide P, Liu L, Sun J, He A, Luscinskas FW, Shi GP. Regulation of endothelial cell adhesion molecule expression by mast cells, macrophages, and neutrophils. *PLoS One*. 2011; 6(1):e14525. doi: 10.1371/journal.pone.0014525.
32. Saghir SA, Al-Gabri NA, Ali AA, Al-Attar AS, Al-Sobarry M, Al-shargi OY, Alotaibi A, Al-zharani M, Nasr FA, Al-Balagi N, Abdulghani MA. Ameliorative effect of thymoquinone-loaded PLGA nanoparticles on chronic lung injury induced by repetitive intratracheal instillation of lipopolysaccharide in rats. *Oxidative Medicine and Cellular Longevity*. 2021 May 28;2021. DOI: 10.1155/2021/5511523
33. Hu H, Li H. Prunetin inhibits lipopolysaccharide-induced inflammatory cytokine production and MUC5AC expression by inactivating the TLR4/MyD88 pathway in human nasal epithelial cells. *Biomed Pharmacother*. 2018; 106:1469-1477. doi: 10.1016/j.biopha.2018.07.093.
34. Yanagihara K, Seki M, Cheng PW. Lipopolysaccharide induces mucus cell metaplasia in mouse lung. *American journal of respiratory cell and molecular biology*. 2001 Jan 1;24(1):66-73. doi.org/10.1165/ajrcmb.24.1.4122
35. Monção-Ribeiro LC, Cagido VR, Lima-Murad G, Santana PT, Riva DR, Borojevic R, Zin WA, Cavalcante MC, Riça I, Brando-Lima AC, Takiya CM, Faffè DS, Coutinho-Silva R. Lipopolysaccharide-induced lung injury: role of P2X7 receptor. *Respir Physiol Neurobiol*. 2011; 179(2-3):314-325. doi: 10.1016/j.resp.2011.09.015.
36. Gholamnezhad Z, Safarian B, Esparham A, Mirzaei M, Esmaeilzadeh M, Boskabady MH. The modulatory effects of exercise on lipopolysaccharide-induced lung inflammation and injury: A systemic review. *Life Sci*. 2022; 293:120306. doi: 10.1016/j.lfs.2022.120306.
37. Ali FF, Abdel-Hamid HA, Toni ND. H2S attenuates acute lung inflammation induced by administration of lipopolysaccharide in adult male rats. *Gen Physiol Biophys*. 2018; 37:421-431. doi: 10.4149/gpb\_2018002.

38. Scalavino V, Liso M, Cavalcanti E, Gigante I, Lippolis A, Mastronardi M, Chieppa M, Serino G. miR-369-3p modulates inducible nitric oxide synthase and is involved in regulation of chronic inflammatory response. *Sci Rep.* 2020; 10(1):15942. DOI: 10.1038/s41598-020-72991-8
39. Li J, Lu K, Sun F, Tan S, Zhang X, Sheng W, Hao W, Liu M, Lv W, Han W. Panaxydol attenuates ferroptosis against LPS-induced acute lung injury in mice by Keap1-Nrf2/HO-1 pathway. *J Transl Med.* 2021; 19(1):96. DOI: 10.1186/s12967-021-02745-1
40. Gupta I, Sehgal R, Kanwar RK, Punj V, Kanwar JR. Nanocapsules loaded with iron-saturated bovine lactoferrin have antimicrobial therapeutic potential and maintain calcium, zinc and iron metabolism. *Nanomedicine (Lond).* 2015; 10(8):1289-1314. DOI: 10.2217/nnm.14.209
41. Drago-Serrano ME, de la Garza-Amaya M, Luna JS, Campos-Rodríguez R. Lactoferrin-lipopolysaccharide (LPS) binding as key to antibacterial and antiendotoxic effects. *Int Immunopharmacol.* 2012; 12(1):1-9. DOI: 10.1016/j.intimp.2011.11.002
42. Hu P, Zhao F, Wang J, Zhu W. Lactoferrin attenuates lipopolysaccharide-stimulated inflammatory responses and barrier impairment through the modulation of NF- $\kappa$ B/MAPK/Nrf2 pathways in IPEC-J2 cells. *Food & function.* 2020; 11(10):8516-8526. DOI: 10.1039/d0fo01570a
43. Lu J, Francis J, Doster RS, Haley KP, Craft KM, Moore RE, Chambers SA, Aronoff DM, Osteen K, Damo SM, Manning S, Townsend SD, Gaddy JA. Lactoferrin: A Critical Mediator of Both Host Immune Response and Antimicrobial Activity in Response to Streptococcal Infections. *ACS Infect Dis.* 2020; 6(7):1615-1623. DOI: 10.1039/d0fo01570a
44. Liu J, Huang X, Hu S, He H, Meng Z. Dexmedetomidine attenuates lipopolysaccharide induced acute lung injury in rats by inhibition of caveolin-1 downstream signaling. *Biomed Pharmacother.* 2019; 118:109314. DOI: 10.1016/j.biopha.2019.109314
45. Li R, Kowalski PS, Morselt HWM, Schepel I, Jongman RM, Aslan A, Ruiters MHJ, Zijlstra JG, Molema G, van Meurs M, Kamps JAAM. Endothelium-targeted delivery of dexamethasone by anti-VCAM-1 SAINT-O-Somes in mouse endotoxemia. *PLoS One.* 2018; 13(5):e0196976. DOI: 10.1371/journal.pone.0196976
46. Chen Y, Wu H, Nie YC, Li PB, Shen JG, Su WW. Mucoactive effects of naringin in lipopolysaccharide-induced acute lung injury mice and beagle dogs. *Environ Toxicol Pharmacol.* 2014; 38(1):279-287. DOI: 10.1016/j.etap.2014.04.030
47. Wang X, Li Q, Li W, Zhang T, Li X, Jiao Y, Zhang X, Jiang J, Zhang X, Zhang X. Dexamethasone attenuated thoracic aortic aneurysm and dissection in vascular smooth muscle cell Tgfbr2-disrupted mice with CCL8 suppression. *Exp Physiol.* 2022; 107(6):631-645. DOI: 10.1113/EP090190
48. Kozan A, Kilic N, Alacam H, Guzel A, Guvenc T, Acikgoz M. The Effects of Dexamethasone and L-NAME on Acute Lung Injury in Rats with Lung Contusion. *Inflammation.* 2016; 39(5):1747-1756. DOI: 10.1007/s10753-016-0409-0

## المخلص العربي

## اللاكتوفيرين مقابل الديكساميثازون في نموذج لإصابة الرئة الحادة في الفئران البالغة: دراسة نسيجية وهستوكيميائية مناعية

بريهان علاء مرزوق، حنان علاء الدين صالح، دعاء رمضان صادق

قسم قسم الهستولوجيا، كلية الطب، جامعة عين شمس

**الخلفية:** يرتبط التعرض المحلي لـ عديد السكاريد الدهني بإنتاج السيتوكين بواسطة الرئة، مما يؤدي إلى ارتشاح العدلات وإصابة الرئة الحادة وهي واحدة من أخطر الأمراض التي تؤثر على الرئتين. خلال جائحة كوفيد-19، أصيب العديد من المرضى بالالتهاب الرئوي الحاد وفي النهاية فشل الرئة. اللاكتوفيرين هو بروتين سكري يرتبط بالحديد وقد يكون له خصائص مضادة للالتهابات.

**الهدف من العمل:** تقييم التأثيرات العلاجية المحتملة للديكساميثازون مقابل اللاكتوفيرين على بنية الرئة في نموذج عديد السكاريد الدهني الناجم عن إصابة الرئة الحادة في الجرذان البالغة.

**المواد والطرق:** تم تقسيم خمسة وثلاثين ذكوراً من الجرذان البيضاء البالغة عشوائياً إلى أربع مجموعات. المجموعة الأولى (مجموعة التحكم)، المجموعة الثانية (مجموعة عديد السكاريد الدهني)، المجموعة الثالثة (مجموعة عديد السكاريد الدهني + اللاكتوفيرين) المجموعة الرابعة (مجموعة عديد السكاريد الدهني + الديكساميثازون). بعد 24 ساعة من حقن كل من اللاكتوفيرين و الديكساميثازون تمت معالجة عينات الرئة للهيماوكسيلين والايوسين ، وحمض شيف الدوري ،والأورسين، والتولويدين الأزرق، والتفاعل الكيميائي المناعي لأكسيد النيتريك المحفز. كما تم إجراء التحليلات المورفومترية والإحصائية.

**النتائج:** أظهرت المقاطع للهيماوكسيلين والايوسين من المجموعة الثانية سماكة ملحوظة في الحاجز بين الحويصلات الهوائية مع تسلل الخلايا الالتهابية الثقيلة (العدلات والبلاعم). بدت معظم الحويصلات الهوائية ضيقة ومتهتكه. تم الكشف عن زيادة كبيرة في متوسط عدد الخلايا الكأسية والخلايا البدينة. ولوحظ أيضاً خلل في الألياف المرنة. كما تم اكتشاف زيادة كبيرة في التفاعل مع الأجسام المضادة لأكسيد النيتريك المحفز. من ناحية أخرى، أظهرت بنية الرئة في المجموعة الثالثة والمجموعة الرابعة تحسناً كبيراً في جميع المعايير.

**الاستنتاج:** أظهر كل من اللاكتوفيرين والديكساميثازون تأثيرات علاجية ومضادة للالتهابات في إصابة الرئة الحادة الناجم عن عديد السكاريد الدهني. وكانت هذه التأثيرات أكثر وضوحاً في الديكساميثازون مقارنة باللاكتوفيرين كما تم اكتشافها من خلال الدراسات المجهرية والمورفومترية والإحصائية.